Journal of Drug Delivery Science and Technology 95 (2024) 105608

Contents lists available at ScienceDirect

Journal of Drug Delivery Science and Technology

journal homepage: www.elsevier.com/locate/jddst

Short communication

Surface modification of titanium foams for modulated and targeted release of drug-loaded biocompatible hydrogel. Proof of concept

Hanaa Mehdi-Sefiani [a,b,*], V.M. Perez-Puyana [b], Ranier Sepúlveda [a], Alberto Romero [b], Juan Dominguez-Robles [c], E. Chicardi [a]

[a] Department of Engineering and Materials Science and Transportation, University of Seville, Seville, Spain
[b] Department of Chemical Engineering, Faculty of Chemistry, University of Seville, Seville, Spain
[c] Pharmacy and Pharmaceutical Technology, Faculty of Pharmacy, University of Seville, Seville, Spain

ARTICLE INFO

Keywords:
Gelatin based-hydrogel
Ti foams
Thermal oxidation
Acid etching
Infiltration
Drug-delivery

ABSTRACT

Bone-tissue replacement surgeries usually need medication to mitigate implant rejections or prevent local infections. In this study, a modulated and targeted tetracycline (TC) loaded gelatine type A hydrogel is release from Ti foams as a proof of concept for an innovative and intelligent drug release system. The drugs are released in a localized and controlled manner. The Ti foams fabricated by the space holder technique were surface modified by two different techniques of surface modification, i.e., thermal oxidation and acid etching, to assess their influence on TC release. The characterization carried out after the surface modification indicated that samples modified with acid etching have produced a rougher surface, increasing the diameter of pores (from 500 μm to 700 μm, approximately) due to coalescence of pores. The increase of pore roughness has demonstrated the delaying of the TC release due to the greater adhesion between the surface roughness and the hydrogel. In addition, the increase of pore size improves the possibility to infiltrate high amount of drug-loaded biocompatible hydrogel. Opposite, oxidized surface samples have generated a rutile type TiO_2 layer that, because of its hydrophilic nature facilitate the degradation of the hydrogel, and consequently, the TC release from the Ti foams. Therefore, both methods show opposite behaviour, available to increase (acid etching) or decrease (thermal oxidation) the TC release thanks to the different kinetic degradation of hydrogel, as a potential way for drug-release from metallic implants. Thus, while acid-etched samples showed maximum TC release value of 35 wt%, after 120 min, the oxidized samples surpassed the 40 % of TC release after same 120 min of release time treatment.

1. Introduction

Currently, titanium and its alloys, mainly the Ti6Al4V, have proven to be the materials of choice for permanent replacement of bone tissue due to their excellent biocompatibility properties, corrosion resistance and relative, but not low enough, modulus of elasticity [1], which play a key role to restore mechanical function by mimicking the mechanical properties of the natural bone tissues [2]. In addition, one of the many positive aspects that make the Ti being the best option over the other metallic biomaterials is the possibility to decrease its Young's modulus being close to the value of bone, avoiding a decrease in the mechanical stress and preventing the stress-shielding effect which causes bone resorption and the loose of the implant [3,4] On the contrary, they are bioinert material, a property that hinders rapid and optimal osseointegration and, therefore, the fixation of the implant with the surrounding bone tissue, which can lead to premature failure due to micromovements [5].

However, Ti and its alloys, analogous to other biomaterials, are usually recognized as foreign materials for the human body and cause an initial response of the host that is currently combated by the administration of drugs such as antibiotics and/or anti-inflammatories [6]. Unfortunately, this type of administration is not efficient due to its undesired side effects, such as toxicity or suboptimal delivery [7].

At present, a tendency to achieve proper administration is to obtain long-acting drug delivery systems, which are able of providing sustained and/or local drug delivery, thus contributing to improve the success of the bone replacement and patient compliance [8–10]. In this sense, hydrogels are three-dimensional crosslinked hydrophilic polymeric networks that are capable of absorbing and retaining significant amounts of water or biological fluids without being dissolved

* Corresponding author. Department of Engineering and Materials Science and Transportation, University of Seville, Seville, Spain.
E-mail address: hanmehsef@alum.us.es (H. Mehdi-Sefiani).

https://doi.org/10.1016/j.jddst.2024.105608
Received 8 January 2024; Received in revised form 2 February 2024; Accepted 19 March 2024
Available online 29 March 2024

themselves [11,12]. Thus, due to the high-water content and the physiochemical similarity to the native extracellular matrix, hydrogels can be used to dissolve and to sustain drug delivery. Considering their high biocompatibility and biocompatibility, these materials can be very valuable also as drug delivery platform [13–16]. In a previous work, Mehdi-Sefiani et al. [17] infiltrated Ti foams with a drug-loaded biocompatible hydrogel achieving controllable drug release.

In this sense, we must be able to improve the local immune environment and promote angiogenesis and osteogenesis that take advantage of osteointegration [18]. For this purpose, a gradual and sustained drug release method must be modulated to solve two aspects: a) the initial acute inflammatory process just after surgery caused by the implant and bone manipulation and the presence of bacteria and b) the persistent inflammation process due to the release of ions, the lack of osteointegration and biocompatibility which may induce periprosthetic osteolysis, loss of bony support subsequent loosening, and failure of the implant [6,19].

The development of osteoimmunology gives us an inspiration that we can properly modify the implants and modulate the local excessive inflammatory response to avoid undesirable lack of osseointegration and improve the patients' quality of life after surgery [18]. Several surface modification techniques have been studied with the aim of altering, in a controlled manner, the topography, surface energy, wettability, as well as biological properties [5,20,21] of Ti foams. Conventional surface treatment methods include thermal oxidation and acid etching. Thermal oxidation consists of generating an oxide film (TiO_2) that has good biocompatibility and stable chemical properties thus optimizing bioactivity, corrosion resistance and osteointegration behaviour of titanium implants [22–24]. On the other hand, acid etching creates a surface of greater roughness that improves cell proliferation and differentiation, in addition to providing a relatively greater bone-implant contact, improved bone growth and improved osseointegration of experimental titanium orthopedic implants [25].

In this work we show an approach to adapt the novel targeted release of drug-loaded biocompatible hydrogel to different drug release kinetic by physical and chemical surface modification on Ti foams generated by space holder technique. Concretely, we present the fundamentals for two surface modification treatments, i.e., conventional thermal oxidation in static air and acid etching with sulfuric acid in Ti foams to modulate and target the release of drug (tetracycline, TC)-loaded biocompatible hydrogel, previously infiltrated in the Ti foams.

2. Materials and methods

2.1. Fabrication and characterization of the Ti foams

Six samples of Ti foams (cylinders with 15 mm height and 12 mm diameter) were prepared with 60 vol% of nominal porosity by space-holder technique to infiltrate type-A gelatin-based hydrogels. This study has used elemental titanium (99% purity, <325 mesh, Strem Chemicals, Newburyport, MA, USA) as metallic material and sodium chloride, NaCl (99.9% purity, <35 mesh, 500 micros, Panreac Química S.L.U., Barcelona, Spain), as the space holder particles. The manufacturing process of Ti foams is described in more detail by Mehdi-Sefiani et al. [17]. In brief, the elemental titanium and sodium chloride NaCl, as the space holders, were mixed in the corresponding volumetric percentage (60 vol% NaCl-40 vol% Ti). The mixture of powders was homogenized and subsequently compacted by uniaxial pressing at 400 MPa. The green compacted cylinders obtained were immersed in hot distilled water to promote the dissolution of the NaCl space-holder. Finally, these developed green Ti foams were then sintered at 1300 °C during 1 h.

The absolute density, open and closed porosities of the samples was calculated by the Archimedes method for porous metallic materials (ASTM B962-17). On the other hand, X-ray diffraction (XRD) patterns were collected for the superficially modified and the non-modified (known as Ti60) samples by thermal oxidation technique to elucidate the nature of the TiO_2 film generated. An image analysis was carried out to determine the morphology, the distribution of pore size and the pore size average by the determination of the circular equivalent diameter of pores (Deq). Cross-section and longitudinal images were obtained using a Nikon Eclipse MA100 N optical microscope. In turn, Image J software was used to analyze these images.

2.2. Surface modification of Ti foams by thermal oxidation

The thermal oxidation procedure was performed in an atmosphere of static air using a CARBOLYTE STF 15/75/450 tubular furnace. The temperature at which the oven was maintained to generate the desired TiO_2 layer in the sample was determined by two previous studies: 1) Hanaor et al. [26] reported that temperatures close to 600 °C, two mechanisms intervene: the diffusion of oxygen in the titanium subnet through the free surface and thorough the grain limits, thereby increasing the volume of TiO_2 and the anatase-rutile transformation takes place; 2) Ma et al. [23] reported that when the temperature is between 675 °C and 750 °C, a rapid oxidation rate and a porous TiO_2 layer are obtained. For all those reasons abovementioned, the temperatures selected were 600 °C, for a total of 25 h and 750 °C, for 2 h (samples labelled as 3MOX600/25 and MOX750/2, respectively). To calculate the oxidation rate obtained after thermal oxidation, the weight gain, and the different molecular weight between Ti and TiO_2 were used.

2.3. Surface modification of Ti foams by acid etching

The procedure to modify the Ti foams by acid etching involved immersing the foams in H_2SO_4 sulfuric acid solutions at room temperature. The samples were then rinsed completely with stirred distilled water to remove any possible sulphates formed after etching. Finally, the samples were dried at 150 °C in an oven. Two different etching studies were carried out: 1) immersion in sulfuric acid 5 M for 10 h, and 2) immersion in sulfuric acid 5 M for 23 h (samples labelled as MC/10 and MC/23, respectively).

2.4. Synthesis of the type-A gelatin-based hydrogel

To synthesize the hydrogel, type-A gelatin (Bloom 300, protein content >85 wt%) was used as the raw material because of its great biocompatibility and ability to form hydrogels [27]. It was supplied by Sigma Aldrich S.A. (Germany). Specifically, the synthesis of type A gelatin-based hydrogel (3 wt%) consisted of dissolving a type-A gelatin in 30 ml of 0.05 M acetic acid. The solution was then centrifuged at 12, 000 rpm for 7 min at 4 °C [28]. Once the solution was centrifugated, 62.5 mg of tetracycline was added to each 25 ml of supernatant hydrogel. Finally, a gelation process was carried out by keeping the hydrogel infiltrated into the pores of Ti foams in a refrigerator at 4 °C for 2 h.

2.5. Infiltration and release for the drug-loaded type-A gelatin-based hydrogels into the Ti foams

After the surface modifications, the infiltration and subsequent release of the tetracycline by relaxation of protein chains of hydrogel in the open porosity of the six Ti foams was carried out. Then, variations in the infiltration and degradation process due to the presence of surface modifications were studied.

The infiltration process was carried out by capillarity with the immersion of each foam in 25 ml of hydrogel for 30 min at room temperature. Subsequently, the samples were placed into a refrigerator at 4 °C for 24 h to allow the gelation of the tetracycline-loaded hydrogel within the pores of Ti foams while it was still infiltrating. The hydrogel was infiltrated in the volume of the open porosity of each sample. The volume of infiltrated hydrogel was calculated by the weight gain of the

Ti foam before and after the infiltration. Once the volume of infiltrated hydrogel was known, the amount of tetracycline release was studied.

To perform the release study, a calibration line was previously established. In particular, the study consisted in immersed each sample in 25 ml of PBS (Phosphate Buffer Solution) and the absorbance was measured with a wavelength of 356 nm. Measurements were taken every 5 min up to 2 h.

In addition, the mechanism of the drug release was modelled following the equation for polymeric systems defined by Korsmeyer et al. [29] (Equation (1)):

$$L = k \bullet t^n \quad (1)$$

where **L** is the degradation's system and **t** the duration of the degradation. From this equation, two important parameters have been obtained: the degradation mechanism that was taking place (**n**) and its kinetics (**k**))

3. Results and discussion

3.1. Characterization of the Ti foams as fabricated

The density and porosity characterization of the six Ti foams, determined by geometry and Archimedes methods are displayed in Table 1. The theoretical density of full dense Ti equal to 4.5 (g cm^{-3}) was used for the relative densification and porosity. Particularly, the percentage of total open and closed porosities, as key parameter for later infiltration and release of TC loaded hydrogel were determined using the Archimedes method, are also displayed in Table 1.

It can be observed how the absolute density on both methods is lower than the density of titanium at room temperature (4.5 g cm^{-3}). This fact is due to the presence of high porosity in Ti foams. Specifically, the percentage of total porosity obtained in both processing conditions is close to the nominal designed (60 vol %). The slight reduction of the total porosity in comparison with the 60 vol% of nominal porosity is caused by the shrinkage during the sintering step. It is noteworthy, as the most important key parameter, the high open porosity in Ti foams (48.4 ± 3.1 vol%), due to this, the 3% hydrogel will be infiltrated, and the tetracycline released by the hydrogel degradation. On the other hand, it can be noted that the values of the relative densification obtained of each sample are within the appropriate range for porous titanium implants (30%–85%) [30].

3.2. Characterization of the Ti foams after surface modification

The oxidation rate for the thermal oxidation was determined according to the weight gain of the two samples, labelled as MOX600/25 and MOX750/2, attending to the oxidation temperature (600 °C and 700 °C) and the oxidation time (25 h and 2 h) applied. As can be highlighted in Fig. 1, the oxidation rate of the Ti foams follows a linear behaviour for the MOX750/2 and a logarithmic growth for the MOX600/25 specimens, respectively, suggesting a non-passivation of the Ti foams. This unusual aspect for Ti, is a consequence of the high specific surface of the Ti foams and the inherent generated microporosity for powder metallurgy materials synthesized and sintered at relative low sintering temperature (1300 °C) that assist the diffusion of oxygen into the Ti foams. This aspect is interesting for this surface modification because of the great control of the oxidation progress. Furthermore, this observation suggests that the TiO_2 layer generated is, in fact, a porous layer. Also, this could be interesting attending to the bioactivity of TiO_2, because the greater the surface area of TiO_2 generated, the more bioactive the surface-modified Ti foam will become. In addition, it is clearly observed that the oxidized sample at 750 °C for 2 h (MOX750/2) reached an oxidation percentage higher than the oxidized sample at 600 °C for 25 h (MOX600/25 h) at lower oxidation time. This indicated that the temperature is the parameter which had the biggest impact on the growth rate of the TiO_2 layer.

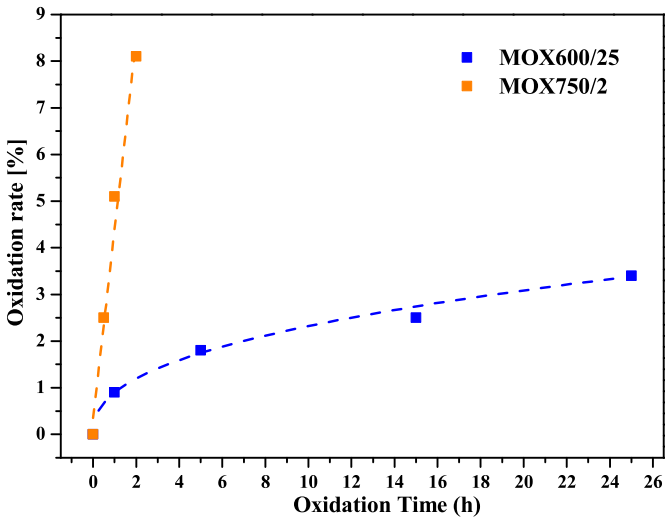

Fig. 1. Oxidation rate of MOX600 and MOX750 samples.

Once the oxidation percentage of each sample was known, the absolute density and porosity of the samples were determined again using the Archimedes method (Table 1). The results shown that the porosity values, mainly the open porosity, of Ti foams before and after thermal oxidation (specimens MOX600/25, MOX750/2 and Ti60 in **Table 1**) are similar, within the standard deviation (48.4 ± 3.1 for Ti60 sample before oxidation vs 52.7% and 46.5% for MOX600/25 and MOX750/2 after oxidation tests). Note that we are focusing the comparison on the open porosity because is the key porosity for the infiltration and releasing process of the drug-loaded hydrogel.

On the other hand, analyzing the results of the samples before and after acid etching, also displayed in Tables 1 and it can be noted that the MC/10 sample had not undergone significant changes in the percentage of total and open porosities after 10 h of acid etching, in comparison with the unmodified sample (51.7 vol % vs 50.5 vol% for total porosity and 49.3 vol% vs 48.4 vol% for open porosity) suggesting a low effect on the percentage of the designed porosity. However, it can be highlighted

Table 1
Density and porosity characterization of as fabricated and surface modified Ti foams determined by geometry and Archimedes method.

System	Absolute density	Relative densification[a]	Total porosity (%)	Open porosity	Closed porosity
	(g·cm^{-3})	(%)		(%)	(%)
Ti60 (Geometry)	1.9 ± 0.1	41.7 ± 2.3	58.3 ± 2.3	ND[b]	ND[b]
Ti60 (Archimedes)	2.3 ± 0.3	50.1 ± 3.9	50.5 ± 3.9	48.4 ± 3.1	1.5 ± 0.5
MOX600/25	2.1	46.5	53.5	52.7	0.8
MOX750/2	2.3	50.9	49.1	46.5	2.6
MC/10	2.2	48.3	51.7	49.3	2.4
MC/23	1.9	35.1	64.9	63.0	1.9

[a] Relative densification %: Percentage of the porous foam density related to bulk titanium's density.
[b] ND: Not Determined.

an increase of open porosity after acid etching for the MC/23 sample. Concretely, from 48.4 ± 3.1 for Ti60 to 63.0 for MC/23 sample. This observation suggests an excessive corrosion on Ti foams, that indicates that if it is necessary to control the increased open porosity of the sample, it is required to control the time when the sample is exposed to sulfuric acid [31].

Subsequently, an XRD analysis was carried out throughout in a radial and longitudinal internal section of the most oxidized sample (MOX750/2) before and after the surface modification to corroborate the successfully formation of the TiO2 layer and its nature (Fig. 2). It is possible to verify the presence of the allotropic rutile phase (titanium oxide, *r*-TiO_2, ref. no. 00-021-1276 in the PDF4+-ICDD database, with tetragonal structure) only after surface modification. For both, the unmodified sample (Ti60) and MOX750/2, the majority phase corresponds to the expected elemental hexagonal close-packed Ti (ref. no. 00-044-1294 in the PDF4+ ICDD database). This fact suggest that thermal oxidation method is able to generate a titanium oxide layer at the surface of the pore's channels of the Ti foams.

To determine the extension of the rutile type titanium oxide layer thickness generated in the MOX600/25 and MOX750/2 samples, an optical microscope image analysis was performed. The optical micrographs shown in Fig. 3 revealed that MOX75O/2 sample had a greater thickness of *r*-TiO_2 compared to the thickness of the MOX600/25 sample. Average values of 8.7 ± 1.8 μm and 16.8 ± 8.1 μm were determined for a high number of measurements in at least 10 micrographs for the MOX600/25 and MOX750/2, respectively.

The pore size distribution was determined using image software and by the determination of the equivalent diameter, defined as the diameter of a circle with an equal area than the pore channel, which is calculated by:

$$d = 2\sqrt{Area/\pi}$$

Where "*d*" is the equivalent diameter (μm) and "*Area*" is the surface of the pore.

The results of the equivalent diameter show that the pore size of the higher oxidized MOX750/2 sample in comparison with the lower oxidized MOX600/25 and with the non-oxidized experiment are similar, between 426 and 457 μm (see Table 2). This fact suggests low influence of the micrometric thickness of the *r*-TiO_2 layers on the submillimetric equivalent diameter of pore size after oxidation stage. On the other hand, analyzing the acid etched samples it can be noted that there has been an increase in the average pore size, more pronounced for high corrosion level (MC/23). This observation in the pore size of the MC/23 can be attributed to the pore coalescence due to the removal of Ti walls

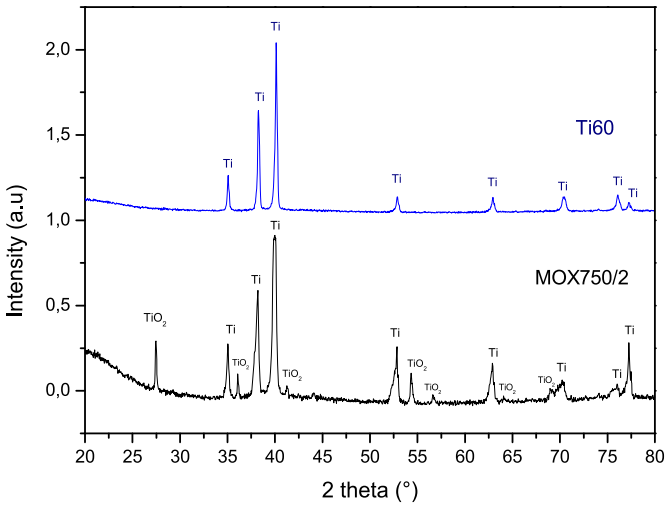

Fig. 2. X-Ray Diffraction patterns for Ti60 and MOX750/2.

that separates the pores, by corrosion [32]. This aspect is demonstrated by the optical micrographs shown in Fig. 4, where the coalescence of pores is exposed (marked with white squares) and, consequently, the increase of pores size for the specimens modified by acid etching in comparison with the not modified Ti60 sample.

Thus, from a surface modified Ti foam design point of view, the space holder selected to generate the porosity could be selected according to the desired final pore size, similar space holder size for oxidized surface modification method and lower space holder size when acid etching is used to modify the surface.

Finally, to determine de effect of the acid etching on the roughness of the walls of the porosity channels generated, a relationship has been obtained between the perimeter of these pores and their surfaces. Higher perimeter/surface relationship is an indirect measurement of higher roughness. Thus, for the Ti60, MC/10 and MC/23 de results obtained are shown in Table 2. Those results indicate that sample MC/10 has the highest roughness due to the higher perimeter-surface ratio. In addition, the sample MC/23 has lower value than the MC/10, probably due to the increase of pore size because of the high corrosion surface treatment time. This aspect can be observed also qualitatively attending to Fig. 5, where it is clearly observed a higher roughness for the MC/10 specimen.

Analogously, the perimeter/surface ratio of pores was determined for the oxidized specimens to corroborate the assertion. In this case, the values obtained are close to the non-modified Ti60 specimens, suggesting no effect of roughness on the behaviour of MOX600/25 and MOX750/2 in comparison with the Ti60 (See Table 2).

Finally, it is important to note that the external morphology and size of all specimens remained invariant after both thermal oxidation and acid etching surface modifications.

3.3. Infiltration-degradation for the gelatin-based hydrogel into the Ti foams

Once the hydrogel was manufactured, it was infiltrated into Ti foams. It is important to note that the percentage of the infiltrated hydrogel was lower than 100% in all the samples (Table 2). This aspect suggests a requirement to use an assisted way to infiltrate all the porosity. As a possibility, the pressure infiltration assisted has been proposed and it will be applied in the following works. After the infiltration process, the tetracycline release was analyzed for all the specimens, i.e., the unmodified sample and the surface modified specimens by both oxidation and corrosion treatments. The release of TC is exposed in Fig. 6 related to the maximum infiltrated hydrogel for each specimen.

Related to the TC release, it is observed as a general trend that, after 120 min, the TC release was incomplete in all cases, i.e., for the as-developed Ti60 specimen and the acid etching and oxidized surface modification specimens. The maximum TC release from the total infiltrated was around 60% for the oxidized MOX750/2 specimen. This aspect suggests that for the purpose to reach the total TC release in a shorter time it should be necessary to address new systems modification.

By other hand, by comparison of the Ti60 and the surface modified specimens by the two ways, i.e., oxidation and acid etching, it is observed how both samples performed by acid etching surface modification exhibited a more sustained release than the rest of the samples. Particularly marked the difference and sustained release for the MC/10 specimen. Not in vain, the maximum TC release for this specimen after 120 min was 25% of TC. The increase on the roughness, indirectly measured by the relationship between the perimeters and the area of pores, determined by Image Analysis, was obtained for this MC/10 specimen (0.045 mm^{-1}) in comparison with the MC/23 (0.040 mm^{-1}) and the non-modified Ti60 (0.033 mm^{-1}). This observation can be attributable to a higher roughness, a higher surface for physical adhesion between hydrogel and Ti foam. Thus, this increase in the surface by roughness improves the bioactivity of Ti foams [32,33], resulting in an increase of hydrogel-Ti interaction and, consequently, delaying and controlling the hydrogel degradation and the subsequent TC releasing.

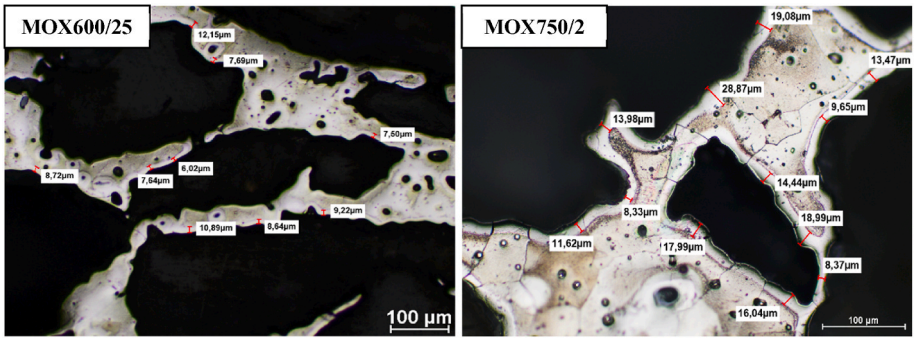

Fig. 3. Comparison of TiO_2 layer thickness of MOX600/25 and MOX750/2 samples.

Table 2
Pore equivalent diameter (D_{eq}) distribution, average perimeter/area ratio of porosity, volume of open porosity, volume of infiltrated hydrogel and percentage of infiltrated hydrogel on the pores for all specimens.

System	D_{eq} [µm]	Perimeter/ Area ratio (mm^{-1})	Volume of open porosity (mL)	Volume infiltrated hydrogel (mL)	Infiltrated hydrogel (%)
Ti60	423 ± 41	0.033	0.688	0.410	59.7
MOX600/25	457 ± 30	0.035	0.759	0.546	71.9
MOX750/2	426 ± 43	0.032	0.611	0.418	68.4
MC/10	667 ± 6	0.045	0.658	0.494	75.1
MC/23	730 ± 42	0.040	0.591	0.391	66.1

In addition, the presence of the roughness produced slower kinetics and lower amounts of drug because, in the infiltration process, the roughness blocked the hydrogel at the beginning of the pore channel, complicating further infiltration. In the degradation process, the roughness prevented a quick interaction between the hydrogel and the PBS, so the degradation of hydrogel and, consequently, the release of TC became slower. On the contrary, an opposite effect can be detected when the surface modification was carried out by static air oxidation. In this case, the presence of the rutile layer formed after oxidation produced an increase in the kinetic degradation of the hydrogel and the TC release, more abruptly when higher thickness of the rutile layer was formed. The hydrophilic nature of the rutile TiO_2 layer [34] could assist the degradation of the hydrogel and, consequently, the interaction between the PBS solution and the hydrogel, achieving faster degradation of hydrogel and, consequently, the increase of release of TC from the Ti foams. Thus, although the presence of both surface modification (acid etching and oxidation) is reported to increase the necessary bioactivity of titanium [23] for the use of Ti foams as bone replacement implants, if they are using also as localized drug delivery system, both surface modification showed opposites behaviour.

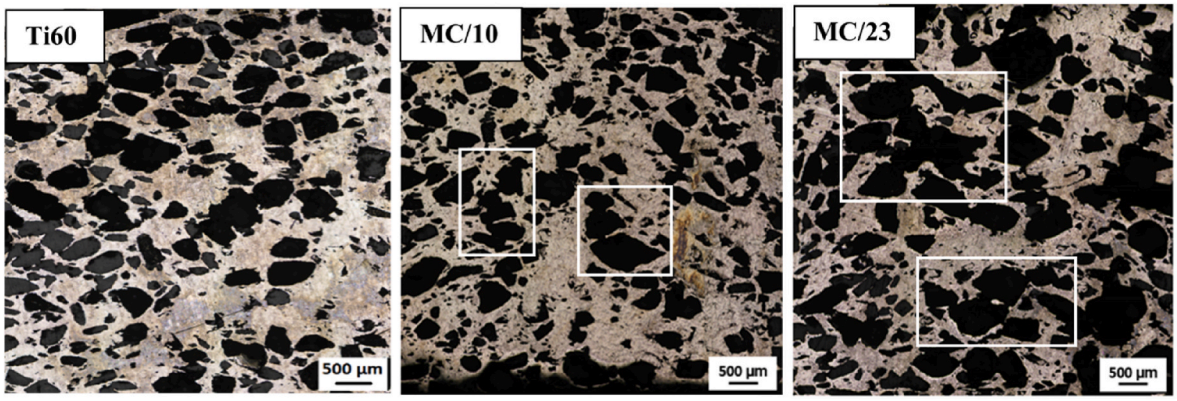

Fig. 4. Optical Micrographs for Ti60 and surface modified MC/10 and MC/23 specimens. Marked by white squares the coalescence of pores.

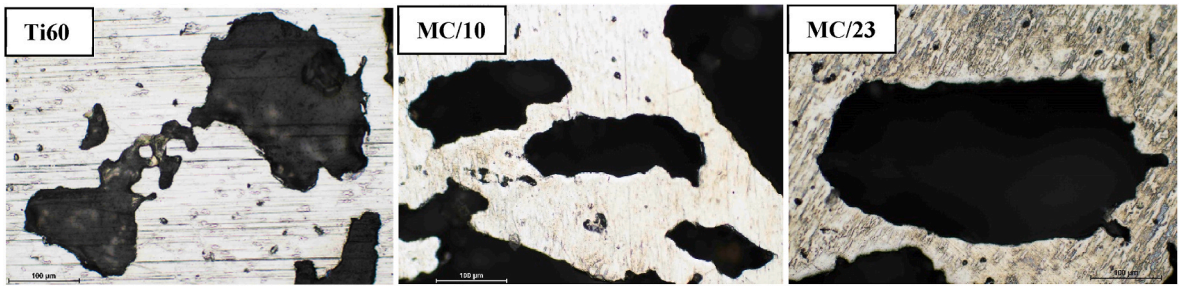

Fig. 5. Pore roughness of acid-etched samples. For comparison purposes, Ti60 it is also showed.

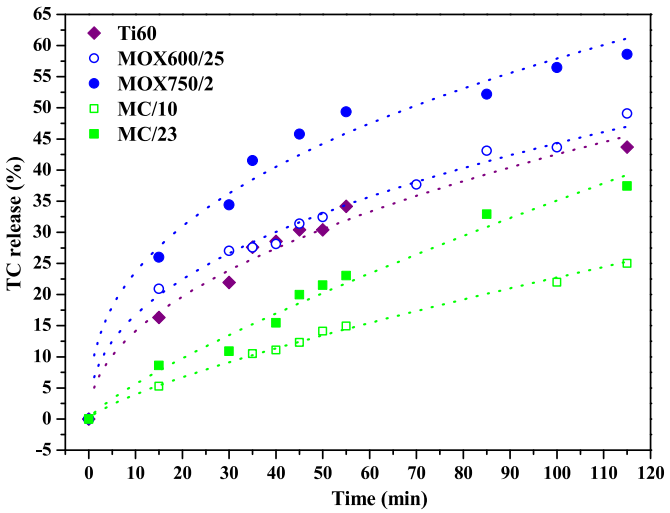

Fig. 6. Kinetic for the TC release from the Ti foams by the hydrogel degradation.

The kinetic data obtained from the potential allometric equation (Table 3), gives "n" exponent similar for the oxidized surface specimens (MOX600/25 and MOX750/2), close to n = 0.40. According to Korsmeyer et al. [29] and Lee [35], this value of n < 0.5 correspond to a typical Fickian diffusion law mechanism caused by the concentration gradient of TC. As opposite, for the acid etching surface modified specimens, the n exponent gives values between 0.5 and 1. In that case, as it was reported by Lee and Korsmeyer [29,35], the mechanism of drug release is an anomalous mechanism, combination of the usual Fickian diffusion mechanism and the swelling process mechanism, based the last one on the relaxation of hydrogel chains due to the water, expansion of chains and, consequently, diffusion of TC and, finally, the total degradation of hydrogel. This observation is in concordance with the higher percentage of TC release level for the oxidize surface specimens. Thus, it is suggested that the hydrophilic nature of the rutile TiO_2 assists the interaction of hydrogel-PBS solution and, consequently, the diffusion of TC from the hydrogel to the PBS solution is caused by a concentration gradient. For this reason, for the thermally oxidized samples, the diffusion mechanism is the clear predominant kinetic mechanism. Opposite, the presence of the roughness in the acid etched surface specimens produced certain degradation of the hydrogel, which induced the release of TC to be carried out by both the degradation of the hydrogel and the diffusion of TC, corroborating the combined mechanism of TC release.

It is important to note that for the non-surface modified specimen (Ti60) the release mechanism for TC release is also the Fickian diffusion mechanism. This fact can be explain considering that, during sintering step, always a nano Ti60 layer is created for Ti, more similar to the oxidized than the acid etched specimens.

Finally, the kinetic constant is an order of magnitude larger for the oxidized surface samples in comparison with the acid etched surface samples, corroborating the higher oxidation rate for the first one as could be abovementioned.

4. Conclusions

In this study two surface functionalization of Ti foams have been successfully implemented, concretely, static air oxidation at high temperature and acid etching. This process has been carried out to understand how to modulate and targeted release of drug-loaded biocompatible hydrogel from the pore channels of modified Ti foams as a vehicle for a controlled and localized release of the drugs required after bone replacement surgery. Thus, the thermal oxidation method has produced a rutile titanium oxide layer that increase the kinetic release of the tetracycline thanks to the analogous hydrophilic nature of rutile TiO_2 layer and the hydrogel as vehicle for the drug-load.

Table 3
Fitting of TC release data from the hydrogel infiltrated in the Ti foam systems.

System	Kinetic constant, k (min^{-n})	Exponent, *n*	R
Ti60	4.7	0.48	0.980
MOX600/25	6.3	0.42	0.993
MOX750/2	9.6	0.39	0.993
MC/10	0.7	0.76	0.993
MC/23	0.9	0.80	0.996

On the other hand, using the acid etching method allow to get a slower tetracycline release from the Ti foams the hydrogel. In fact, the samples' kinetic release profiles showed that due to the presence of roughness, the interaction of the pore surface with the hydrogel increases and therefore, the release of the drug slows down.

Finally, it is important to highlight that this study is a proof of concept so it can be noted some improvements. For example, the percentage of the hydrogel infiltrated was lower than 100% in all the samples so, for future studies related to this work could be important the use of pressure to allow a completed infiltration. On the other hand, related to the time of drug release, it could be necessary to modify the hydrogel to provide it with optimal rheological properties that could allow to achieve an extending longer release over time.

CRediT authorship contribution statement

Hanaa Mehdi-Sefiani: Writing – original draft, Visualization, Validation, Software, Investigation, Formal analysis, Data curation, Conceptualization. **V.M. Perez-Puyana:** Writing – original draft, Visualization, Supervision, Resources, Project administration, Methodology, Funding acquisition, Conceptualization, Formal analysis, Validation. **Ranier Sepúlveda:** Writing – review & editing, Visualization. **Alberto Romero:** Writing – review & editing, Visualization. **Juan Dominguez-Robles:** Writing – review & editing, Visualization. **E. Chicardi:** Writing – original draft, Visualization, Validation, Supervision, Resources, Project administration, Methodology, Investigation, Formal analysis, Conceptualization.

Declaration of competing interest

The authors declare that they have no known competing financial interests or personal relationships that could have appeared to influence the work reported in this paper.

Data availability

Data will be made available on request.

Acknowledgements

This study was financially supported by MCIN/AEI/10.13039/501100011033/FEDER, UE, through the project PID2021-124294OB-C21. The authors their financial support. This work was also possible thanks to the postdoctoral contract of Víctor M. Pérez Puyana from the "Contratación de Personal Investigator Doctor" supported by the European Social Fund and Junta de Andalucía (PAIDI DOCTOR – Convocatoria 2019–2020, DOC_00586). Authors would also like to thanks to Ms. Diana Antyukhova Antyukhova and Ms. Sandra Jaramillo-Dorado undergraduate students for their assistance in the surface modification experiments carried out.

References

[1] K.Y. Hung, S.C. Lo, C.S. Shih, Y.C. Yang, H.P. Feng, Y.C. Lin, Titanium surface modified by hydroxyapatite coating for dental implants, Surf. Coat. Technol. 231 (2013) 337–345, https://doi.org/10.1016/j.surfcoat.2012.03.037.

[2] S.L. Sing, J. An, W.Y. Yeong, F.E. Wiria, Laser and electron-beam powder-bed additive manufacturing of metallic implants: a review on processes, materials and designs, J. Orthop. Res. 34 (2016) 369–385, https://doi.org/10.1002/JOR.23075.

[3] Y. Torres, P. Trueba, J.J. Pavón, E. Chicardi, P. Kamm, F. García-Moreno, J. A. Rodríguez-Ortiz, Design, processing and characterization of titanium with radial graded porosity for bone implants, Mater. Des. 110 (2016) 179–187. https://doi:10.1016/J.MATDES.2016.07.135.

[4] A. Rodriguez-Contreras, M. Punset, J.A. Calero, F.J. Gil, E. Ruperez, J.M. Manero, Powder metallurgy with space holder for porous titanium implants: a review, J. Mater. Sci. Technol. 76 (2021) 129–149. https://doi:10.1016/J.JMST.2020.11.005.

[5] Y. Li, Y. You, B. Li, Y. Song, A. Ma, B. Chen, W. Han, C. Li, Improved cell adhesion and osseointegration on anodic oxidation modified titanium implant surface, J. Hard Tissue Biol. 28 (2019) 13–20, https://doi.org/10.2485/jhtb.28.13.

[6] K.M.R. Nuss, B. von Rechenberg, Biocompatibility issues with modern implants in bone - a review for clinical orthopedics, Open Orthop. J. 2 (2008) 66, https://doi.org/10.2174/1874325000802010066.

[7] S. Saghazadeh, C. Rinoldi, M. Schot, S.S. Kashaf, F. Sharifi, E. Jalilian, K. Nuutila, G. Giatsidis, P. Mostafalu, H. Derakhshandeh, K. Yue, W. Swieszkowski, A. Memic, A. Tamayol, A. Khademhosseini, Drug delivery systems and materials for wound healing applications, Adv. Drug Deliv. Rev. 127 (2018) 138–166, https://doi.org/10.1016/j.addr.2018.04.008.

[8] E. Larrañeta, T. Raghu Raj Singh, R.F. Donnelly, Overview of the clinical current needs and potential applications for long-acting and implantable delivery systems, Long-Acting Drug Delivery Systems: Pharmaceutical, Clinical, and Regulatory Aspects (2022) 1–16, https://doi.org/10.1016/B978-0-12-821749-8.00005-7.

[9] S.A. Stewart, J. Domínguez-Robles, R.F. Donnelly, E. Larrañeta, Implantable polymeric drug delivery devices: classification, manufacture, materials, and clinical applications, Polymers 10 (2018) 1379, https://doi.org/10.3390/POLYM10121379, 10 (2018) 1379.

[10] J. Domínguez-Robles, E. Utomo, V.A. Cornelius, Q.K. Anjani, A. Korelidou, Z. Gonzalez, R.F. Donnelly, A. Margariti, M. Delgado-Aguilar, Q. Tarrés, E. Larrañeta, TPU-based antiplatelet cardiovascular prostheses prepared using fused deposition modelling, Mater. Des. 220 (2022) 110837, https://doi.org/10.1016/J.MATDES.2022.110837.

[11] K. Peng, L.K. Vora, J. Domínguez-Robles, Y.A. Naser, M. Li, E. Larrañeta, R. F. Donnelly, Hydrogel-forming microneedles for rapid and efficient skin deposition of controlled release tip-implants, Mater. Sci. Eng. C 127 (2021) 112226, https://doi.org/10.1016/J.MSEC.2021.112226.

[12] J. Maia, M.P. Ribeiro, C. Ventura, R.A. Carvalho, I.J. Correia, M.H. Gil, Ocular injectable formulation assessment for oxidized dextran-based hydrogels, Acta Biomater. 5 (2009) 1948–1955, https://doi.org/10.1016/J.ACTBIO.2009.02.008.

[13] M. McKenzie, D. Betts, A. Suh, K. Bui, L.D. Kim, H. Cho, Hydrogel-based drug delivery systems for poorly water-soluble drugs, Molecules 20 (2015) 20397–20408, https://doi.org/10.3390/molecules201119705.

[14] M.C. Catoira, L. Fusaro, D. Di Francesco, M. Ramella, F. Boccafoschi, Overview of natural hydrogels for regenerative medicine applications, J. Mater. Sci. Mater. Med. 30 (2019), https://doi.org/10.1007/s10856-019-6318-7.

[15] T.R. Hoare, D.S. Kohane, Hydrogels in drug delivery: progress and challenges, Polymer 49 (2008) 1993–2007, https://doi.org/10.1016/j.polymer.2008.01.027.

[16] N.H. Thang, T.B. Chien, D.X. Cuong, Polymer-based hydrogels applied in drug delivery: an overview, Gels 9 (2023), https://doi.org/10.3390/gels9070523.

[17] H. Mehdi-Sefiani, V. Perez-Puyana, F.J. Ostos, R. Sepúlveda, A. Romero, M. Rafii-El-Idrissi Benhnia, E. Chicardi, Type-A gelatin-based hydrogel infiltration and degradation in titanium foams as a potential method for localised drug delivery, Polymers 15 (2023), https://doi.org/10.3390/polym15020275.

[18] W. Liu, M. Yu, F. Chen, L. Wang, C. Ye, Q. Chen, Q. Zhu, D. Xie, M. Shao, L. Yang, A novel delivery nanobiotechnology: engineered miR-181b exosomes improved osteointegration by regulating macrophage polarization, J. Nanobiotechnol. 19 (2021) 269, https://doi.org/10.1186/s12951-021-01015-y.

[19] E. Gibon, L.A. Córdova, L. Lu, T.H. Lin, Z. Yao, M. Hamadouche, S.B. Goodman, The biological response to orthopedic implants for joint replacement. II: polyethylene, ceramics, PMMA, and the foreign body reaction, J. Biomed. Mater. Res. B Appl. Biomater. 105 (2017) 1685–1691, https://doi.org/10.1002/jbm.b.33676.

[20] T. Jemt, M. Olsson, V. Franke Stenport, Incidence of first implant failure: a retroprospective study of 27 Years of implant operations at one specialist clinic, Clin. Implant Dent. Relat. Res. 17 (2015) e501–e510, https://doi.org/10.1111/cid.12277.

[21] G. Wang, J. Li, K. Lv, W. Zhang, X. Ding, G. Yang, X. Liu, X. Jiang, Surface thermal oxidation on titanium implants to enhance osteogenic activity and in vivo osseointegration, Sci. Rep. 6 (2016), https://doi.org/10.1038/srep31769.

[22] M.T. Mohammed, Z.A. Khan, A.N. Siddiquee, Surface modifications of titanium materials for developing corrosion behavior in human body environment: a review, Procedia Materials Science 6 (2014) 1610–1618, https://doi.org/10.1016/j.mspro.2014.07.144.

[23] K. Ma, R. Zhang, J. Sun, C. Liu, International Journal of Corrosion 2020 (2020), https://doi.org/10.1155/2020/1678615.

[24] S. Sangeetha, S. Kathyayini, P. Deepak Raj, P. Dhivya, M. Sridharan, Biocompatibility studies on Ti02 coated Ti surface, in: Proceedings of the International Conference on 'Advanced Nanomaterials and Emerging Engineering Technologies- ICANMEET 2013, 2013, pp. 404–408, https://doi.org/10.1109/ICANMEET.2013.6609330.

[25] H. Saksø, T. Jakobsen, M. Saksø, J. Baas, S. Jakobsen, K. Soballe, No positive effect of acid etching or plasma cleaning on osseointegration of titanium implants in a canine femoral condyle press-fit model, Open Orthop. J. 7 (2013) 1–7, https://doi.org/10.2174/1874325001307010001.

[26] D.A.H. Hanaor, C.C. Sorrell, Review of the anatase to rutile phase transformation, J. Mater. Sci. 46 (2011) 855–874, https://doi.org/10.1007/S10853-010-5113-0.

[27] A. Ahmady, N.H. Abu Samah, A review: gelatine as a bioadhesive material for medical and pharmaceutical applications, Int. J. Pharm. 608 (2021) 121037, https://doi.org/10.1016/J.IJPHARM.2021.121037.

[28] V. Perez-Puyana, M. Jiménez-Rosado, A. Romero, A. Guerrero, Fabrication and characterization of hydrogels based on gelatinised collagen with potential application in tissue engineering, Polymers 12 (2020), https://doi.org/10.3390/POLYM12051146.

[29] R.W. Korsmeyer, R. Gurny, E. Doelker, P. Buri, N.A. Peppas, Mechanisms of solute release from porous hydrophilic polymers, Int. J. Pharm. 15 (1983) 25–35, https://doi.org/10.1016/0378-5173(83)90064-9.

[30] K. Pałka, R. Pokrowiecki, Porous titanium implants: a review, Adv. Eng. Mater. 20 (2018) 18, https://doi.org/10.1002/ADEM.201700648.

[31] T.T. Nguyen, A. Miller, M.F. Orellana, Characterization of the porosity of human dental enamel and shear bond strength in vitro after variable etch times: initial findings using the BET Method, Angle Orthod. 81 (2011) 707, https://doi.org/10.2319/083010-506.1.

[32] D.J. Fernandes, R.G. Marques, C.N. Elias, Influence of acid treatment on surface properties and in vivo performance of Ti6Al4V alloy for biomedical applications, J. Mater. Sci. Mater. Med. 28 (2017), https://doi.org/10.1007/s10856-017-5977-5.

[33] A. Jemat, M.J. Ghazali, M. Razali, Y. Otsuka, Surface modifications and their effects on titanium dental implants, BioMed Res. Int. 2015 (2015), https://doi.org/10.1155/2015/791725.

[34] R.S. Mane, O.S. Joo, S.K. Min, C.D. Lokhande, S.H. Han, A simple and low temperature process for super-hydrophilic rutile TiO 2 thin films growth, Appl. Surf. Sci. 253 (2006) 581–585, https://doi.org/10.1016/j.apsusc.2005.12.123.

[35] P.I. Lee, Kinetics of drug release from hydrogel matrices, J. Contr. Release 2 (1985) 277–288, https://doi.org/10.1016/0168-3659(85)90051-3.